

TAILORING THE PROPERTIES OF COMPOSITE PIEZOELECTRIC MATERIALS  
FOR MEDICAL ULTRASONIC TRANSDUCERS

Wallace Arden Smith and Avner Shaulov  
Philips Laboratories, North American Philips Corporation, Briarcliff Manor, New York 10510

B.A. Auld  
Edward L. Ginzton Laboratories, Stanford University, Stanford, California 93405

Abstract

Transducers for medical ultrasonic imaging have been made from composite piezoelectric materials. This paper describes a simple physical model for the material properties which govern the thickness-mode oscillations in thin plates of PZT-rod/polymer composites. We consider the case where the lateral periodicity of the rods is much smaller than all relevant acoustic wavelengths. Expressions are derived for the effective material parameters in terms of the properties of the constituents. The composites' properties can then be tailored to device requirements by choosing appropriate components and by varying the volume fraction of piezoceramic. Our analysis reveals the need for a trade-off between the desired lower acoustic impedance and the undesired smaller electromechanical coupling that occurs as the volume fraction of piezoceramic is reduced. The predictions of this model are in good agreement with measurements made on rod-composite plates containing 5 to 35 percent PZT.

1. Introduction

A variety of composite piezoelectric materials can be made by combining a piezoelectric ceramic with a passive polymer phase [1-3]. These new piezoelectrics greatly extend the range of material properties offered by the conventional piezoelectric ceramics and polymers. Recently, such composite piezoelectrics have found fruitful application in transducers for pulse-echo medical ultrasonic imaging [4-7]. These transducers were made from PZT-rod/polymer composites which are shown schematically in Figure 1.

The piezoelectric used in ultrasonic transducers should have a high electromechanical coupling coefficient,  $k_t$ , to efficiently convert between electrical and mechanical energy. An acoustic impedance,  $Z$ , close to that of tissue (1.5 Mrayl) is desired so that the acoustic waves in the transducer and tissue couple well both during transmission and reception. A dielectric constant,  $\epsilon^S$ , that is reasonably large ( $> 100$ ) facilitates electrical matching to the driving and receiving electronics. Low electrical losses ( $\tan\delta < 0.05$ ) and low mechanical losses ( $Q_m > 10$ ) are also important for high sensitivity.

Conventional piezoelectric ceramics (lead zirconate-titanate, lead metaniobate and modified lead titanates) only partially meet these needs. They offer high electromechanical coupling ( $k_t \sim 0.4 - 0.5$ ), a wide selection of dielectric constants ( $\epsilon^S \sim 100 - 2400$ ) and low electrical and mechanical losses ( $\tan\delta < 0.02$ ,  $Q_m \sim 10 - 1000$ ). The major drawback is their high acoustic impedance ( $Z \sim 20-30$  Mrayl). On the other hand, the low acoustic impedance ( $Z \sim 4$  Mrayl) of piezoelectric polymers (polyvinylidene difluoride and its copolymer with trifluorethylene) makes acoustic matching easy. However, their low electromechanical coupling ( $k_t < 0.3$ ) and high dielectric losses ( $\tan\delta \sim 0.15$ ) limit the sensitivity; moreover, the polymers' low dielectric constant ( $\epsilon^S \sim 10$ ) places severe demands on the transmitter and receiver electronics.

Composite piezoelectrics provide properties superior to both the ceramics and polymers. Coupling constants can be larger ( $k_t \sim 0.6-0.75$ ) than those of the ceramics, while the acoustic impedance is much lower ( $Z < 7.5$  Mrayl) - reaching the range of the piezopolymers. The composites also provide a wide range of dielectric constants ( $\epsilon^S \sim 10 - 1000$ ) and low dielectric and mechanical losses.

This paper presents a theoretical model for these material parameters of PZT-rod/polymer composites which allows us to optimize the properties of these composite piezoelectrics.

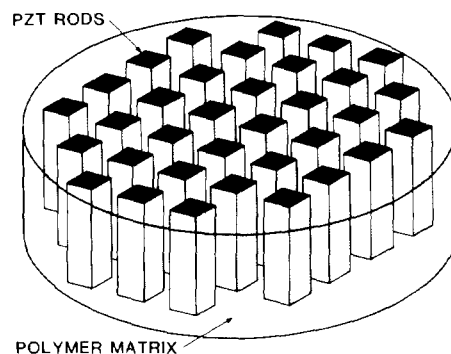


Figure 1. Schematic representation of PZT-rod/polymer composite

## 2. Composite Spatial Scale

We shall model the composite piezoelectrics as an effective homogeneous medium. The detailed microstructure of the composite and the different properties of the constituent phases are subsumed in the averages taken to calculate the behavior of the new medium. When can we treat the composite as a homogeneous medium? Clearly not always since the lateral periodicity of the rods gives rise to a rich set of phenomena reflecting the composite's microstructure [8-12]. In particular, the composite's microstructure appears whenever lateral running waves on these composite plates are resonantly reflected by the lateral periodicity of the rod spacing. Whenever the periodicity of these Lamb waves matches that of the composite microstructure stop bands appear in the Lamb wave dispersion curves. Such stop bands introduce resonances in the response of the composite medium that invalidate the treatment as a homogeneous medium.

Figure 2a provides a schematic representation of the Lamb wave dispersion curves for an isotropic homogeneous medium. These curves show the angular frequency,  $\omega$ , versus wavenumber,  $\beta$ , for running waves on a plate. The heavy black dot on the vertical axis (i.e.  $\beta = 0$ ) represents the longitudinal thickness resonance in this plate. Figures 2b and 2c show the modifications to Figure 2a produced by resonant reflections in the periodic structure of the composite. The dashed vertical lines identify the wavelengths which are resonantly reflected by the periodic lattice of rods. In Figure 2b the rod periodicity is rather coarse and the lateral stop band resonances occur for frequencies near that of the fundamental thickness resonance. Figure 2c corresponds to a rod composite with fine lateral spatial scale; here, lateral stop-band resonances occur only at frequencies much higher than the thickness-mode resonance.

In medical ultrasound transducers only a band of frequencies near the thickness-mode resonance is used. Thus, if the lateral spatial scale is sufficiently fine, a composite can be effectively represented as a homogeneous medium. We restrict ourselves to spatial scales within this regime.

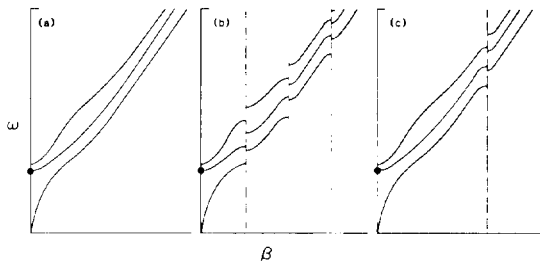


Figure 2. Schematic representation of Lamb wave dispersion curves for (a) a homogeneous plate, (b) a composite plate with coarse lateral periodicity and (c) a composite plate with fine lateral periodicity. The large dot denotes the thickness-mode resonance.

## 3. Constitutive Relations

This section presents a simple physical model for the material parameters which govern the thickness-mode resonance in PZT-rod/polymer composites. Our model follows the spirit of the parallel connectivity [13] picture used to calculate composite properties. Since we focus only on thickness-mode oscillations of thin plates of rod composites, substantial simplifications are achieved. Moreover, our sharp focus allows us to treat an important physical effect - the lateral stresses generated within these plates - by means of a simple physical approximation.

Our goal is to calculate the effective constitutive relations for this medium. We choose the strains and electric field as the independent coordinates and orient the composite plate in the x-y plane with the fundamental repeats of the rod lattice lying along these axes. We take the piezoelectric ceramic to be poled along the rods - perpendicular to the plate.

As a first physical approximation, we assume that the strains and electric field are independent of x and y throughout the individual phases. These fields still, of course, vary along the z direction. Adding the usual simplifications made in analyzing the thickness mode oscillations in a large, thin plate (symmetry in x-y plane,  $E_1 = E_2 = 0$ , etc.), we can write down the constitutive relations for the individual phases. Namely, within the polymer ("p") phase, we have,

$$\begin{aligned} T_1^D &= (c_{11} + c_{12}) S_1^D + c_{12} S_3^D \\ T_3^D &= 2 c_{12} S_1^D + c_{11} S_3^D \\ D_3^D &= \epsilon_{11} E_3^D \end{aligned} \quad (1)$$

while within the ceramic ("c") phase, we have,

$$\begin{aligned} T_1^C &= (c_{11}^E + c_{12}^E) S_1^C + c_{13}^E S_3^C - e_{31} E_3^C \\ T_3^C &= 2 c_{13}^E S_1^C + c_{33}^E S_3^C - e_{33} E_3^C \\ D_3^C &= 2 e_{31} S_1^C + e_{33} S_3^C + \epsilon_{33}^S E_3^C \end{aligned} \quad (2)$$

The elastic and dielectric constants of the ceramic phase are distinguished from those of the polymer phase by the superscripts E and S, respectively.

In describing the coupling of the phases, a key approximation embodies our picture that the ceramic and polymer move together in a uniform thickness oscillation. Thus the vertical strains are the same in both phases, namely,

$$S_3^D(z) = S_3^C(z) = \bar{S}_3(z) \quad (3)$$

This is valid when the composite has such fine spatial scale that stop-band resonances are at much higher frequencies than the thickness resonance.

In relating the electric fields in the two phases, we shall neglect all fringing fields and take the electric fields to be the same in both phases, namely,

$$E_3^D(z) = E_3^C(z) = \bar{E}_3(z) \quad (4)$$

This is not a critical approximation. Indeed, since the dielectric constant of a piezoceramic is several hundred times that of a polymer, we might even totally neglect the polymer phase for volume fractions of piezoceramic greater than a percent.

A crucial approximation addresses the lateral interaction between the phases. We assume that the lateral stresses are equal in both phases and that any lateral strain in the ceramic is compensated by a complimentary strain in the polymer. Then the composite as a whole is laterally clamped although the individual phases are not, so we have,

$$T_1^D(z) = T_1^C(z) = \bar{T}_1(z) \quad (5)$$

$$\bar{S}_1(z) = (1 - v) S_1^D(z) + v S_1^C(z) = 0$$

where  $v$  is the volume fraction of piezoceramic.

This assumption about the lateral motion permits us to express the lateral strains in terms of the vertical strain and electric field as,

$$S_1^C = -\frac{c_{13}^E - c_{12}}{c(v)} \bar{S}_3 + \frac{e_{31}}{c(v)} \bar{E}_3 \quad (6)$$

$$S_1^D = \frac{\alpha(v) (c_{13}^E - c_{12})}{c(v)} \bar{S}_3 - \frac{\alpha(v) e_{31}}{c(v)} \bar{E}_3$$

where  $c(v) = c_{11}^E + c_{12}^E + \alpha(v) (c_{11} + c_{12})$  and  $\alpha(v) = v/(1-v)$ .<sup>11</sup> We can use these expressions to eliminate the lateral strains from the constitutive relations and obtain  $T_3^D$ ,  $D_3^D$ ,  $T_3^C$  and  $D_3^C$  in terms of  $\bar{S}_3$  and  $\bar{E}_3$  alone.

Our final approximation deals with the dependent coordinates. If the lateral periodicity is sufficiently fine, we get the effective total stress and electric displacement by averaging over the contributions of the constituents, namely,

$$\bar{T}_3(z) = v T_3^C(z) + (1-v) T_3^D(z) \quad (7)$$

$$\bar{D}_3(z) = v D_3^C(z) + (1-v) D_3^D(z)$$

So the final constitutive relations take the form,

$$\bar{T}_3 = \bar{c}_{33}^E \bar{S}_3 - \bar{e}_{33} \bar{E}_3$$

$$\bar{D}_3 = \bar{e}_{33} \bar{S}_3 + \bar{\epsilon}_{33}^S \bar{E}_3$$

where

$$\bar{c}_{33}^E = v \left[ c_{33}^E - \frac{2 (c_{13}^E - c_{12})^2}{c(v)} \right] + (1 - v) v_{11}$$

$$\bar{e}_{33} = v \left[ e_{33} - \frac{2 e_{31} (c_{13}^E - c_{12})}{c(v)} \right] \quad (9)$$

$$\bar{\epsilon}_{33}^S = v \left[ \epsilon_{33}^S + \frac{2 (e_{31})^2}{c(v)} \right] + (1 - v) \epsilon_{11}$$

#### 4. Transducer Parameters

Using  $S_3$  and  $E_3$  as independent coordinates is convenient for modeling the composite properties. However, the oscillations in a thin plate are most readily analyzed using  $S_3$  and  $D_3$  as independent coordinates. This change is simple to effect and yields,

$$\bar{T}_3 = \bar{c}_{33}^D \bar{S}_3 - \bar{h}_{33} \bar{D}_3 \quad (10)$$

$$\bar{E}_3 = \bar{h}_{33} \bar{S}_3 + \bar{\beta}_{33}^S \bar{D}_3$$

where

$$\bar{c}_{33}^D = \bar{c}_{33}^E + (\bar{e}_{33})^2 / \bar{\epsilon}_{33}^S \quad (11)$$

$$\bar{h}_{33} = \bar{e}_{33} / \bar{\epsilon}_{33}^S$$

$$\bar{\beta}_{33}^S = 1 / \bar{\epsilon}_{33}^S$$

These relations must be supplemented by the expression for the composite density, namely,

$$\bar{\rho} = v \rho^C + (1 - v) \rho^D \quad (12)$$

Equations (9), (11) and (12) give all the needed parameters of the composite piezoelectric expressed in terms of the properties of the components. We resist writing these expressions in detail, as they are rather unwieldy. Inserting these expressions into the conventional analysis of thickness-mode oscillations in a thin piezoelectric plate we can evaluate the quantities of interest for ultrasonic transducers, namely, the electromechanical coupling constant,

$$\bar{k}_t = \bar{h}_{33} / (\bar{c}_{33}^D \bar{\beta}_{33}^S)^{1/2} = \bar{e}_{33} / (\bar{c}_{33}^D \bar{\epsilon}_{33}^S)^{1/2} \quad (13)$$

the specific acoustic impedance,

$$\bar{z} = (\bar{c}_{33}^D / \bar{\rho})^{1/2} \quad (14)$$

and the longitudinal velocity,

$$\bar{v}_1 = (\bar{c}_{33}^D / \bar{\rho})^{1/2} \quad (15)$$

## 5. Results

To illustrate how the composite material parameters vary with volume fraction of piezoceramic we take the case of PZT5 ceramic [14] and SPURR epoxy [15]. Table 1 contains the material parameters used for this example.

The basic material parameters,  $\bar{\rho}$ ,  $\bar{\epsilon}_{33}^S$ ,  $\bar{C}_{33}^D$ , and  $\bar{e}_{33}$ , are shown in Figure 3. These quantities vary essentially linearly with volume fraction of piezoceramic over most of the range ( $\bar{\rho}$  strictly so, over the entire range). However, as the volume fraction becomes large, the lateral clamping of the rods through the polymer has an appreciable effect on the elastic and piezoelectric behavior: the elastic stiffness,  $\bar{C}_{33}^D$ , increases and the piezoelectric strain constant,  $\bar{e}_{33}$ , decreases.

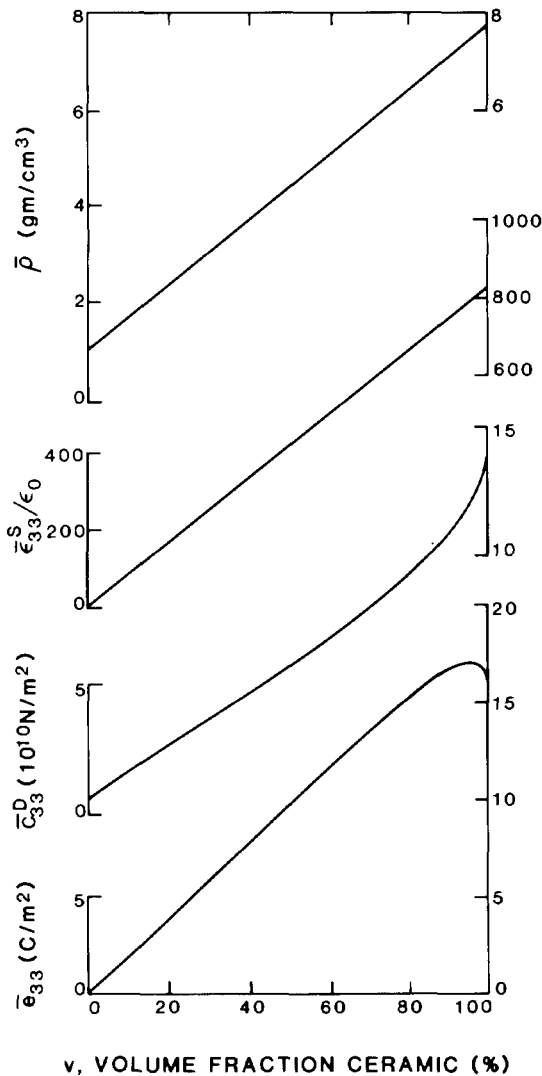


Figure 3. Variation of material parameters of a composite with volume fraction piezoceramic.

These are the principal effects of the lateral stress exerted by the polymer matrix on the piezoceramic rods. This lateral clamping of the rods also diminishes the dielectric constant in this range, but the effect is small. The dielectric constant also deviates from strict proportionality to volume fraction at the low end. But this deviation appears only when  $v$  is well below a percent, and we may ignore it. For small volume fractions, the other quantities also vary essentially linearly with  $v$ , assuming at zero their value in the polymer phase. At zero, the piezoelectric coupling strictly vanishes. The polymer's density and elastic stiffness, though much smaller than the ceramic's (i.e.  $\sim 10\%$ ), are not totally negligible as is the case with the dielectric constant (i.e.  $\ll 1\%$ ).

The behavior of the device parameters,  $\bar{Z}$ ,  $\bar{v}_l$  and  $\bar{k}_t$ , is shown in Figure 4. These variations with volume fraction follow directly from those of the basic material parameters. The acoustic impedance increases essentially linearly with volume fraction, except at the high end where the clamping of the rods causes it to sweep up. The velocity also sweeps up at the high end due to stiffening of

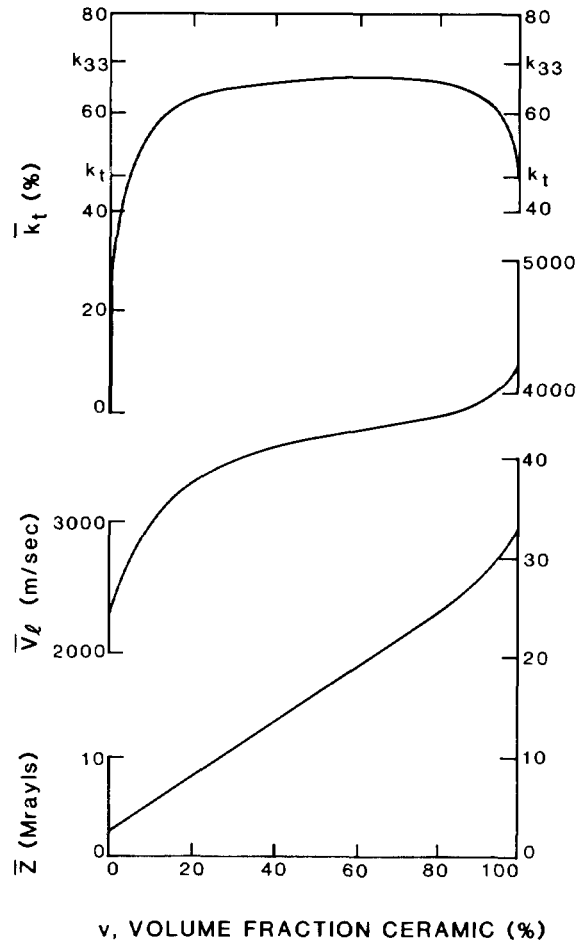


Figure 4. Variation of transducer parameters of a composite with volume fraction piezoceramic.

the rods by lateral forces from the polymer. Also for low volume fractions, the velocity exhibits an interesting variation. As the ceramic fraction increases, the stiffening effect of adding more ceramic is overcome by the concomitant mass loading. The electromechanical coupling constant is nearly the  $k_{33}$  of free ceramic rods except for deviations at low, and high, volume fractions. As the high end is approached, the lateral clamping of the rods by the polymer causes the sharp decrease in  $k_t$  to the value of the coupling constant for a solid ceramic disk,  $k_t$ . For small volume fractions, the elastic loading of the piezoceramic causes the diminution in  $k_t$ ; but at intermediate volume fractions of piezoceramic,  $k_t$  falls below  $k_{33}$  because of both elastic loading and lateral clamping.

For medical imaging transducers, one wants a piezoelectric with low acoustic impedance and high electromechanical coupling. These curves show that rod-polymer composite piezoelectrics can be superior to ceramic piezoelectrics in both respects. The optimum material can be achieved by adjusting the volume fraction of piezoceramic in the composite. Lowering the volume fraction always lowers the acoustic impedance but eventually causes a deterioration in the electromechanical coupling. A trade-off then must be made between minimizing the impedance and maximizing the coupling. Figure 5 illustrates this trade-off between low acoustic impedance and high electromechanical coupling. The solid curve displays the results for PZT5 and SPURR epoxy, while the dotted and dashed curves result from using the material parameters [16] for a soft (polyethylene) and a very stiff (Dow epoxy resin 332, loaded with alumina) polymer phase, respectively. Clearly the softer polymer affords a more favorable trade-off: lower impedances can be achieved with higher coupling constant. The precise trade-off between low  $Z$  and high  $k_t$  requires a Mason-model analysis incorporating specific assumptions about the acoustical and electrical matching to be used in the transducer design.

Table 1. Material parameters of PZT5 [14], SPURR epoxy [15], polyethylene [16] and Dow epoxy resin loaded with alumina [16] used in the examples.

| PZT5                                      |       |                              |      |
|---|-------|------------------------------|------|
| $c_{11}^E$ ( $10^{10}$ N/m <sup>2</sup> ) | 12.1  | $e_{31}$ (C/m <sup>2</sup> ) | -5.4 |
| $c_{12}^E$ ( $10^{10}$ N/m <sup>2</sup> ) | 7.54  | $e_{33}$ (c/m <sup>2</sup> ) | 15.8 |
| $c_{13}^E$ ( $10^{10}$ N/m <sup>2</sup> ) | 7.52  | $\epsilon_{33}^S/\epsilon_0$ | 830  |
| $c_{33}^E$ ( $10^{10}$ N/m <sup>2</sup> ) | 11.1  | $\rho$ (g/cm <sup>3</sup> )  | 7.75 |
|   | SPURR | polyethylene                 | Dow  |
| $v_l$ (m/s)                               | 2200  | 1950                         | 3180 |
| $v_s$ (m/s)                               | 1000  | 540                          | 1620 |
| $\rho$ (g/cm <sup>3</sup> )               | 1.1   | 0.9                          | 1.76 |

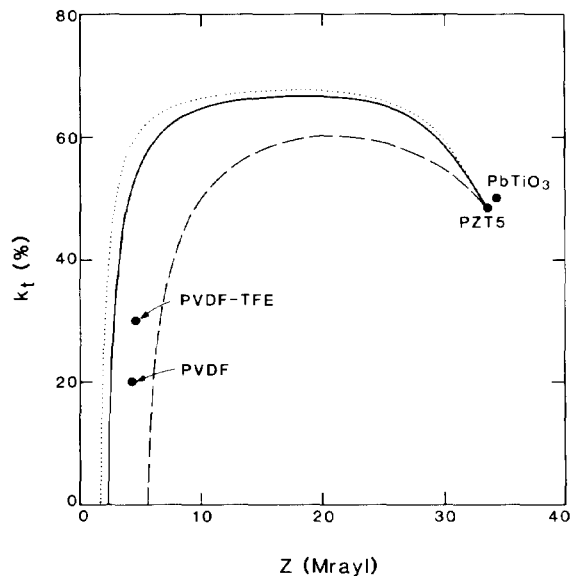


Figure 5. The trade-off between high electromechanical coupling and low acoustic impedance in composite made from PZT5 and SPURR (solid), polyethylene (dotted) or Dow epoxy resin loaded with alumina (dashed).

While a soft polymer provides a favorable  $k_t$ - $Z$  bar trade-off curve, this benefit is not without cost. The softer polymer requires finer lateral spatial scales in the composite structure to avoid unwanted lateral stop-band resonances. Going out of the long-wavelength regime deteriorates the improvements in both impedance matching and electromechanical conversion efficiency.

To test our modeling experimentally, a number of special samples were made from a rather stiff polymer and between 5% and 35% of a PZT5H type ceramic. The stiff polymer was used to emphasize the  $k_t$ - $Z$  trade-off that appears at small volume fraction of ceramic. The material constants of these plates were obtained by measuring the frequency dependence of the electrical impedance in the vicinity of the thickness-mode resonance in thin plates using either the IEEE standard [17] or the impedance circle technique [18]. The acoustic impedance was determined from the measured values of the sound velocity and density. These data are plotted together with the relevant theoretical curves in Figure 6. The elastic properties,  $v_l$  and  $Z$ , agree with the calculation within 6%; this is well within the experimental uncertainties and normal sample-to-sample variations. The electromechanical coupling exhibits the expected variation with volume fraction of PZT, but attains values slightly below the calculated ones. This is understandable since any deviations caused by depoling during fabrication or by inadequate electrical contact will diminish the measured value of  $k_t$ .

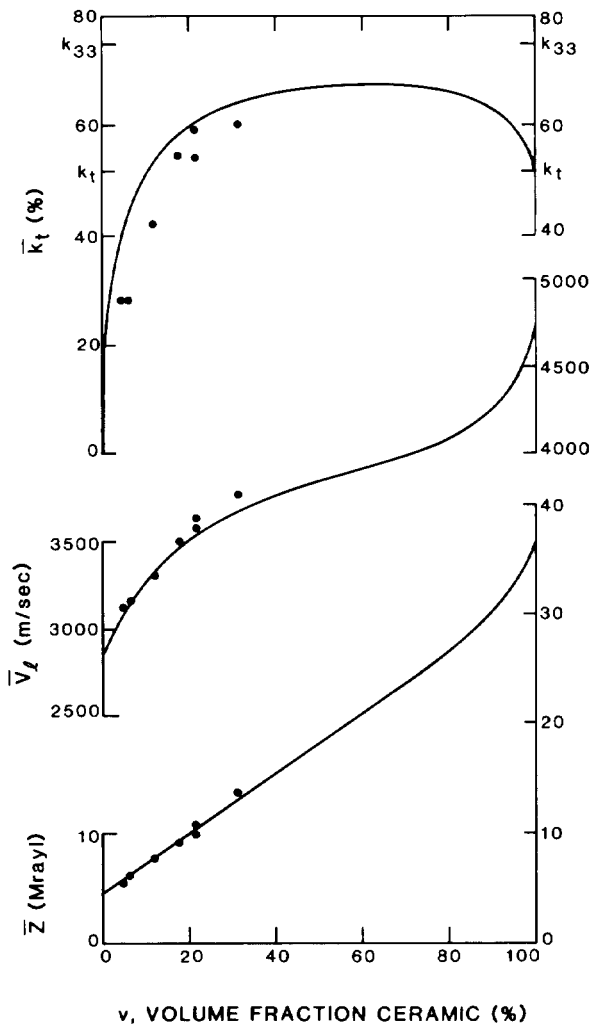


Figure 6. Experimental verification of variations of transducer parameters with volume fraction piezoceramic.

### 6. Conclusions

To make a sensitive, broadband ultrasonic transducer, one wants a piezoelectric with low acoustic impedance,  $Z$ , and high electromechanical coupling,  $k_t$ . PZT-rod/polymer composites can be superior to ceramic piezoelectrics in both respects. The optimum material can be achieved by selecting the piezoceramic and polymer components and by adjusting the volume fraction of piezoceramic. Our theoretical model shows how the electromechanical properties of the composite piezoelectrics vary with constituent properties and with volume fraction of the piezoceramic. Predictions of the model are in good agreement with measurements and reveal that, in optimizing composite transducer performance, a trade-off must be made between minimizing  $Z$  and maximizing  $k_t$ . A softer polymer will yield a more favorable  $k_t - Z$  trade-off curve. However, the softer polymer will require finer lateral spatial scales in the composite structure to remain in the long-wavelength region. Going out of this regime will deteriorate the improvements in both  $k_t$  and  $Z$ .

### 7. Acknowledgments

Helpful discussions with and encouragement by B. Singer are greatly appreciated. We are indebted to M. Athanas, D. Cammack, R. Dalby, D. Dorman, S. Frazier, K. Mc Keon, A. Pink and J. Zola for their contributions in fabrication and measurements.

### 8. References

1. R. E. Newnham, A. Safari, G. Sa-gong and J. Giniewicz, Proc. 1984 IEEE Ultrasonics Symposium 501.
2. A. Safari, R. E. Newnham, L. E. Cross and W. A. Schulze, *Ferroelectrics* 41, 197 (1982).
3. R. E. Newnham, L. J. Bowen, K. A. Klicker and L. E. Cross, *Materials in Engineering* 2, 93 (1980).
4. H. Takeuchi, C. Nakaya and K. Katakura, Proc. 1984 IEEE Ultrasonics Symposium 507.
5. T. R. Gururaja, W. A. Schulze, L. E. Cross and R. E. Newnham, Proc. 1984 IEEE Ultrasonics Symposium 533.
6. W. A. Smith, A. A. Shaulov and B. M. Singer, Proc. 1984 IEEE Ultrasonics Symposium 539.
7. A. A. Shaulov, W. A. Smith and B. M. Singer, Proc. 1984 IEEE Ultrasonics Symposium 545.
8. B. A. Auld, H. A. Kunkel, Y. A. Shui and Y. Wang, Proc. 1983 IEEE Ultrasonics Symp. 554.
9. B. A. Auld, Y. A. Shui and Y. Wang, *Journal de Physique* 45, 159-163 (1984).
10. T. R. Gururaja, W. A. Schulze, L. E. Cross, B. A. Auld, Y. A. Shui and Y. Wang, *Ferroelectrics* 54, 183-186 (1984).
11. T. R. Gururaja, W. A. Schulze, L. E. Cross, R. E. Newnham, B. A. Auld and J. Wang, Proc. 1984 IEEE Ultrasonics Symposium 523.
12. B. A. Auld and Y. Wang, Proc. 1984 IEEE Ultrasonics Symposium 529.
13. R.E. Newnham, D.P. Skinner and L.E. Cross, *Materials Research Bulletin* 13, 525 (1978).
14. D. A. Berlincourt, D. R. Curran and H. Jaffee, in *Physical Acoustics*, Volume 1A, edited by W. P. Mason, Academic Press, 1964.
15. Spurr Low Viscosity Embedding Medium, Polysciences Inc., Warrington, Pennsylvania.
16. A. R. Selfridge, *IEEE Transactions on Sonics and Ultrasonics* SU-32, 381 (1985).
17. IRE Standards on Piezoelectric Crystals, Proc. IRE 49, 1161 (1961).
18. R. Holland and E. P. EerNisse, *IEEE Trans. Sonics Ultrason.* SU-16, 173 (1969).